Eur. Phys. J. D **28**, 267–272 (2004)
DOI: 10.1140/epjd/e2003-00312-5

THE EUROPEAN PHYSICAL JOURNAL D

Optical operation of ultracold atomic quasi-clusters

Wenhua Hai[a], Guishu Chong, Qiongtao Xie, and Jing Lu

Department of Physics, Hunan Normal University, Changsha 410081, P.R. China

Received 6 October 2002 / Received in final form 3 February 2003
Published online 16 December 2003 –

Abstract. We report several exact solutions of a two-dimensional (2D) Gross-Pitaevskii equation with an optical lattice potential, which describe the motion of an array of ultracold atomic quasi-clusters in a Bose-Einstein condensate. The velocity of the atomic quasi-clusters can be controlled by adjusting the optical potential strength so that one can stop or drive them by the optical brake. The atomic quasi-clusters form a superfluid for the propagation state or a critical insulator for the non-propagation one, and the brake and drive are associated with the quantum phase transitions between the insulator and superfluid.

PACS. 03.75.-b Matter waves – 05.70.Jk Critical point phenomena – 05.30.Jp Boson systems – 67.90.+z Other topics in quantum fluids and solids; liquid and solid helium

1 Introduction

The optical lattice potential induced by the ac Stark effect of interfering laser beams has been often used to confine ultracold atoms [1–7]. The corresponding theoretical investigations were carried out by using two different methods. One of them employs the Bose-Hubbard model [8–11] to develop the dynamics of the bosonic atoms on the optical lattices. To derive some useful results from this model, one had to adopt the harmonic approximation expanding around the minima of the potential wells [12,13]. Another method is to consider the mean field approximation [14,15] and to solve the Gross-Pitaevskii equation (GPE) with the optical lattice potential [16–20]. Most of the analytical work was based on a quasi-1D model in the context of ultracold atoms, where the optical lattice potential was applied to study the macroscopic quantum interference [16], atom number squeezing [17], Josephson junction arrays [18] and discrete solitons [19], and so on. Several exact steady state solutions of 1D GPE were constructed and discussed by Bronski et al. [20]. The results were extended to multi-dimensional cases [21], and the stabilities of the exact solutions [22] and interference patterns [23] of the system were demonstrated. The quantum phase transitions between a superfluid and a Mott insulator were theoretically predicted in the Bose-Hubbard model [12,24,25] and experimentally observed by Greiner and coworkers [13] in a Bose-Einstein condensate (BEC) with repulsive interactions, held in a 3D optical lattice potential. It is well-known that the superfluid state can be described by the GPE of mean field theory, but the Mott insulating state cannot. There exist two interesting problems: In what case does the GPE become invalid in the process of quantum transition? Has the system a critical state between the superfluid and Mott insulating states?

Our previous works have investigated the time evolutions of some 3D BECs analytically and numerically [26]. In this paper, we report several exact analytical solutions of the 2D stationary state GPE with either two different or identical component amplitudes of the optical lattice potential and demonstrate that the analytical results indicate a useful method to experimentally operate the ultracold atomic quasi-clusters in the optical lattices. Differing from common atomic clusters that are bound only by the interatomic interactions, formations of the atomic quasi-clusters depend on the external optical lattice potential. According to our analytical results, the atomic quasi-clusters behave like free particles after setting the optical potential to equilibrate the atom-atom interaction. By increasing the depth of the first potential component enough to suppress the quantum tunnel along the first direction, the atomic quasi-clusters are forced to move toward another direction and the problem is reduced to quasi-1D one. Further increasing the depth of the second potential component can stop the atomic quasi-clusters, then decreasing the depth will drive them again. The brake and drive imply the existence of quantum phase transitions between a superfluid and a critical insulator, where the GPE is just validated. The results show that mean field theory is valid only for the ratio of trap depth to interatomic interaction intensity being less than or equal to two times the atomic number per well. When the depth is equal to this limit, the system arrives at the critical insulating state. If the limit is exceeded by the trap depth, the GPE is no longer valid and the system may enter the Mott insulating state. Our critical insulating state is a new one that just gives the critical value of the trap depth for

[a] e-mail: adcve@cs.hn.cn

stopping the atomic quasi-clusters, which should be less than the critical value to enter the Mott insulating state. The result is in qualitative agreement with the experimental data reported by Greiner et al.

2 Exact solutions of the 2D GPE

In the recent experiment of Greiner et al. [13], a 3D optical lattice potential proportional to the product of the dynamic atomic polarizability and the laser intensity within a harmonic potential from magnetic trap were set. The forced radio-frequency evaporation was used to create condensed atoms near a temperature of absolute zero. If we turn off the standing wave laser along the z-direction and adjust the magnetic trap potential to reduce the 3D system to quasi-2D one. Counting in the magnetic contribution, the total 2D potential is written as $V = m\omega^2(x^2 + y^2)/2 + V_1 \sin^2 kx + V_2 \sin^2 ky$, where the term proportional to the atomic mass m is the magnetic potential with ω the trap frequency, k is the wavevector of the laser light, the amplitudes V_1 and V_2 may be the same or different with positive or negative sign. Adopting Greiner's experimental parameters $\omega = 24$, $\lambda = 2\pi/k = 0.852$ μm, $V_1 = V_2 \sim E_r$, $m \approx 87m_p$ with m_p being the proton mass and $E_r = \hbar^2k^2/2m$ the recoil energy, the magnetic potential strengths read as $m\omega^2(x^2 + y^2)/2 = 4.14137 \times 10^{-7}k^2(x^2 + y^2)E_r$. In the experimentally valid region of the magnetic trap, the maximal harmonic potential is much less than the maximal optical one and can be neglected such that we have the stationary state 2D GPE

$$-\psi_{xx} - \psi_{yy} + \left(V_1 \sin^2 x + V_2 \sin^2 y + g_0|\psi|^2\right)\psi = \mu\psi. \quad (1)$$

Here the wave function ψ has been normalized in units of the wavevector k, the spatial coordinate has been normalized by k^{-1}, and the amplitude V_i and chemical potential μ have been normalized by the recoil energy E_r so all variables and parameters in equation (1) are dimensionless. In such units, the interatomic interaction intensity related to the s-wave scattering length a is in the form $g_0 = 8\pi ka$.

It is quite interesting to derive the exact solutions of GPE (1) for describing the ultracold atomic quasi-clusters, whose norm is spatially periodical and phase is nontrivial. Theoretically, equation (1) allows us to select a suitable laser potential such that the two competing potentials, external and internal interactions, reach indifferent equilibrium. This can be experimentally done by adjusting the optical potential to make a balance between it and the interatomic interaction. By using this method, some exact solutions of 1D GPE for a repulsive interaction with $g_0 = 1$ were constructed by Bronski et al. [20]. By the balance between the external and internal interactions we mean that their sum is equal to a constant,

$$V_1 \sin^2 x + V_2 \sin^2 y + g_0|\psi(x, y)|^2 = \mu - 1. \quad (2)$$

Thus equation (1) is simplified to the linear Schrödinger equation of a free particle $\psi_{xx} + \psi_{yy} + \psi = 0$ whose solutions are familiar to us,

$$\begin{aligned}\psi_1 &= R_1 \exp(i\Theta_1) = \sqrt{-V_1/g_0}\sin x + i\sqrt{-V_2/g_0}\sin y \\ &\qquad \text{for } \mu = 1,\ V_i/g_0 < 0; \\ R_1^2 &= -(V_1 \sin^2 x + V_2 \sin^2 y)/g_0, \\ \Theta_1 &= \arctan(\sqrt{V_2}\sin y/\sqrt{V_1}\sin x); \end{aligned} \quad (3)$$

$$\begin{aligned}\psi_2 &= R_2 \exp(i\Theta_2) = \sqrt{V_1/g_0}\cos x + i\sqrt{V_2/g_0}\cos y \\ &\qquad \text{for } \mu = 1 + V_1 + V_2,\ V_i/g_0 > 0; \\ R_2^2 &= (V_1 \cos^2 x + V_2 \cos^2 y)/g_0, \\ \Theta_2 &= \arctan(\sqrt{V_2}\cos y/\sqrt{V_1}\cos x). \end{aligned} \quad (4)$$

The transpositions between x and y in equations (3, 4) can lead to two new solutions $\psi_3 = R_3 \exp(i\Theta_3)$ and $\psi_4 = R_4 \exp(i\Theta_4)$ that have same norms and different phases with the solutions ψ_1 and ψ_2 respectively. The chemical potential μ of the macroscopic quantum system corresponds to the eigenenergy in the Schrödinger equation of a single particle. It may take various possible values representing various possible states of the system. The solutions (3, 4) corresponding to $\mu = 1$ and $\mu = 1 + V_1 + V_2$ denote two special states respectively. They not only satisfy the Schrödinger equation for a free particle, but also obey the constraint of equation (2). The constraint leads the solution to a sum of the cosine and sine terms, as in equations (3, 4). Their exponential forms, $\cos x = (e^{ix} + e^{-ix})/2$, $i \sin x = (e^{ix} - e^{-ix})/2$, show that any exact solution is a linear superposition of four plane waves propagating along $\pm x$- and $\pm y$-directions with velocity μ. Hence these exact solutions are some shape-preserving wave packets and represent several stationary states of the nonlinear Schrödinger equation for a BEC interacting with the standing wave laser field. Their norms denoting the densities of particle number are spatially periodic and therefore describe some arrays of ultracold atomic quasi-clusters. Setting $V_1 = V_2 = 8$ and using the experimental parameters [13] $\lambda = 2\pi/k = 852$ nm, $a = 5.5$ nm, namely $g_0 = 8\pi ka \approx 1.02$, from equation (4) we plot the 2D number density R_2^2 on the xOy-plane in Figure 1, where the mesh surface represents the 2D potential. For the attractive interaction with $g_0 = -1.02$, $V_1 = V_2 = 8$ from equation (3) we make the plot R_1^2 on the xOy-plane in Figure 2. These figures respectively display eight atomic quasi-clusters with density distributions over each optical lattice that are essentially identical.

The total number of the BEC atoms N cannot be strictly fixed in general experiments, because of the loss of atoms. An interesting property is that if N is fixed, any one of the exact solutions allows us to simultaneously know the phase in any jth lattice and the average number of atoms per lattice. For instance, by setting the total number of the optical lattice sites as $n \times n$, the applications of ψ_i with known phase Θ_i to the normalization integral

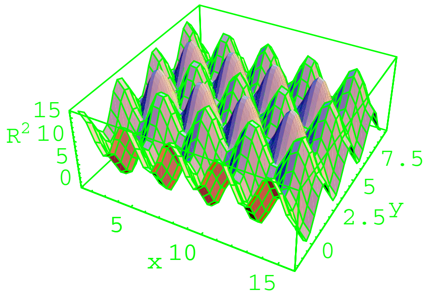

Fig. 1. A 3D plot of the particle number density R^2 on $x\mathrm{O}y$-plane from equation (4) for parameters $V_1 = V_2 = 8$, $g_0 = 1.02$. Eight ultracold atomic quasi-clusters are shown in this figure. The mesh surface represents the 2D optical potential.

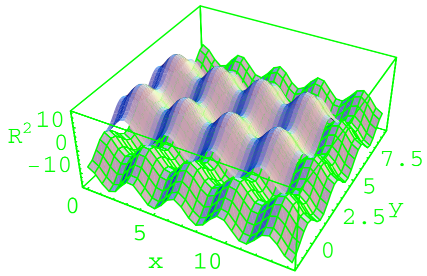

Fig. 2. Surface of the particle number density on $x\mathrm{O}y$-plane from equation (3) with $V_1 = V_2 = 8$ and $g_0 = -1.02$ that exhibits eight different atomic quasi-clusters.

result in the average number of atoms per well

$$N/n^2 = (n\pi)^{-2}\int_{\pi/2}^{(n+1/2)\pi} R_i^2(x,y)dxdy = |(V_1+V_2)/(2g_0)| \quad (5)$$

for $i = 1, 2, 3, 4$, where we have let the boundary coordinate be $x_0 = y_0 = \pi/2$ which is the peak point of the optical potential. For two identical standing waves with $V_1 = V_2 = V_0$ the number becomes $N/n^2 = |V_0/g_0|$. A marvelous property is that when the system is in any state of equations (3, 4), the average number of BEC atoms per well is completely determined by the trap depth $|V_i|$ for the given g_0.

Let the BEC atoms initially fill some optical lattice sites, the ultracold atomic quasi-clusters form and move with a certain velocity on the $x\mathrm{O}y$-plane. The phase gradient of the solution ψ_i is correlated to the superfluid velocity $\vec{v}_i = k\hbar\vec{\nabla}\Theta_i(x,y)/m$ and atomic current density $\vec{J}_i = R_i^2\vec{v}_i$. The appearance of the factor k is due to the normalized coordinates by its inverse, k^{-1}. The spatially dependent propagation velocity and atomic current density imply that the motion of the atomic quasi-clusters is not only a whole translation, but also contains the spatially variable internal-motion. Applying equations (3, 4) we rewrite the atomic current density formula as

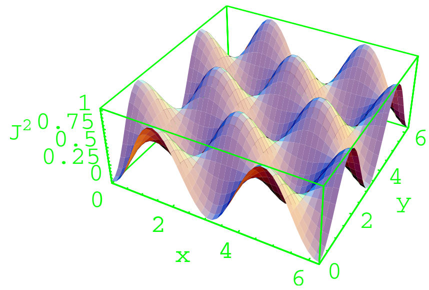

Fig. 3. The norm of current densities on $x\mathrm{O}y$-plane from equation (7) in unit $k^2\hbar^2V_1V_2/(mg_0)$, which shows its spatial periodicity.

$$\vec{J}_i = R_i^2\vec{v}_i = \frac{R_i^2 k\hbar}{m}\left(\frac{\partial\Theta_i}{\partial x}\vec{e}_x + \frac{\partial\Theta_i}{\partial y}\vec{e}_y\right) = \frac{k\hbar\sqrt{V_1V_2}}{mg_0}\vec{e}_i,$$
$$\vec{e}_1 = \vec{e}_4 = (\cos x\sin y\vec{e}_x - \cos y\sin x\vec{e}_y),$$
$$\vec{e}_2 = \vec{e}_3 = (\cos y\sin x\vec{e}_x - \cos x\sin y\vec{e}_y), \quad (6)$$

where $\vec{e}_x$ and $\vec{e}_y$ denote the unit vectors of x and y-directions. It is easily seen that the norms of the four current densities are identical, namely

$$|\vec{J}_i|^2 = J^2 = \frac{k^2\hbar^2V_1V_2}{mg_0}(\cos^2 x\sin^2 y + \cos^2 y\sin^2 x). \quad (7)$$

Adopting the unit $k^2\hbar^2V_1V_2/(mg_0)$, this is plotted in Figure 3, which shows periodical evolutions of the current norm on $x\mathrm{O}y$-plane. Equations (6, 7) show that the amplitude of the current density can be controlled by the trap depth V_i. It warrants our attention that the exact solutions contain the zero density points $(x_0,\ y_0)$ at which $R_i(x_0,\ y_0) = 0$ meaning that no atoms can reach these points. Therefore, at these points the superfluid velocity has no definition.

The Bose-Hubbard Hamiltonian is a representation of the exact Hamiltonian with two-body interactions using the basis of Wannier states, localized at the lattice sites. There are two approximations that give the Bose-Hubbard Hamiltonian:

a. only a single band is assumed;
b. only nearest neighbor interactions are included.

Differing from this, our approach can be used to seek exact solutions of the system without these approximations. Comparing with the atoms in the Bose-Hubbard lattices where one is allowed to create or annihilate a single atom in any lattice for a superfluid, our atomic quasi-cluster can form and propagate as a whole, through the optical operation. Another difference between the Bose-Hubbard model and our method is that the former can be applied to the Mott insulator and the latter can treat only the superfluid and critical insulating state.

It is known that if one suddenly turns off the magnetic and optical trap in an experiment, the atomic wave function will retain its initial phase and exhibit the interference pattern [13,27,28]. From equations (3, 4) we

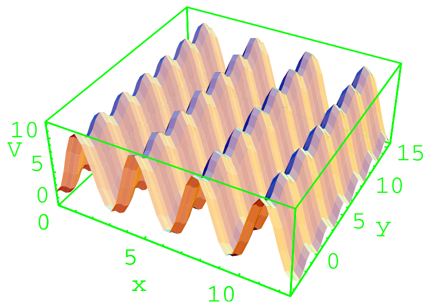

Fig. 4. Surface of the 2D optical potential $V = V_1 \sin^2 x + V_2 \sin^2 y$ on the xOy-plane for $V_1 = 10$ and $V_2 = 2$. It shows that for a sufficiently high barrier V_1 the BEC atoms can propagate only in the y-direction.

have the superposition of two atomic waves coming from different lattice sites with coordinates x, y and x', y',

$$\psi_i(x, y) + \psi_i(x', y') = \exp[i\Theta_i(x, y)] \times \{R_i(x, y) + R_i(x', y') \exp[i\Theta_i(x', y') - i\Theta_i(x, y)]\}. \quad (8)$$

The nontrivial phase difference $\Theta_i(x', y') - \Theta_i(x, y)$ can lead to the interference pattern, as in Greiner et al.'s experiment.

3 Optical operation of the atomic quasi-clusters

In order to operate the 2D atomic quasi-clusters, we require adjustment of the laser potential. For the potential $V(x,\ y) = V_1 \sin^2 x + V_2 \sin^2 y$, it is well-known that sufficiently great well depth $|V_1|$ or $|V_2|$ can suppress the motion in the x- or y-direction and reduces the 2D problem to quasi-1D. This assertion is illustrated numerically in Figure 4, where we have set $V_1 = 10$, $V_2 = 2$ and imposed a high potential barrier in the x-direction. As V_1 is increased to a critical value, no atoms can tunnel through it such that the atomic quasi-clusters propagate only in the y-direction.

In this case, we need only to consider the quasi-1D stationary state GPE in the form

$$-\psi_{yy} + \left[V_2 \sin^2 y + g_0|\psi|^2\right] \psi = \mu\psi. \quad (9)$$

The quasi-1D GPE with the optical lattice potential has been applied to many physical fields [16–19,29]. Adopting a method very similar to the 2D case, making the 1D external potential balance with the interatomic interaction, we derive the 1D superfluid solution

$$\begin{aligned} \psi(y) &= \sqrt{(\mu - 1)/g_0}\ \cos y + i\sqrt{(\mu - 1 - V_2)/g_0}\ \sin y \\ &= R(y) \exp[i\Theta(y)], \\ R(y) &= \sqrt{(\mu - 1 - V_2 \sin^2 y)/g_0}, \\ \Theta(y) &= \arctan\left[\sqrt{1 - V_2/(\mu - 1)}\ \tan y\right]. \end{aligned} \quad (10)$$

Obviously, if the trap depth $|V_2|$ exceeds the constant $|\mu - 1|$, the module and phase of equation (10) cannot be kept as real functions which would make the solution of PGE invalid. Therefore, the maximum and critical trap depth is $|V_2| = |\mu - 1|$ for holding the exact solution. In other words, for a given $|V_2|$ the value of $|\mu - 1|$ is great than or equal to it. To keep positive atomic number density, equation (10) requires that the chemical potential depends on the properties of the interatomic interaction. The attractive interaction with $g_0 < 0$ needs it to obey $\mu - 1 < 0$ and the repulsive one with $g_0 > 0$ limits it to $\mu - 1 > 0$. If one changes the sign of g_0 through the Feshbach resonance [30,31], the transitions occur between the states $\mu - 1 < 0$ and $\mu - 1 > 0$. Letting $g_0 = 1$ and $V_2 = -V_0$, equation (10) becomes the known solution given by Bronski et al. [20].

As in the 2D case, the exact solution (10) describes some stationary states of the 1D nonlinear Schrödinger equation for a BEC interacting with a standing wave laser field. Its norm is spatially periodic and thereby represents an array of BEC atomic quasi-clusters. When one suddenly turns off the magnetic and optical trap in an experiment, the atomic wave function will retain its initial phase and exhibit the interference pattern. The phase gradient $\nabla\Theta(y)$ is correlated to the velocity field $v(y) = k\hbar\Theta_y/m = Ck\hbar/(mR^2)$ and the atomic current density $J = R^2 v = Ck\hbar/m$ with $C = g_0^{-1}\sqrt{(\mu - 1)(\mu - 1 - V_2)}$ being a constant. The constant current density describes an uniform atom current with nonzero flow velocity. This implies that the atomic quasi-clusters can move from one lattice site to the next with a time-independent velocity. If one initially and locally creates a condensate on the side of the optical potential [32], its velocity may be nonzero and toward another side of the potential. Thus the ultracold atomic quasi-clusters form and propagate in that direction. In the presence of a source of ultracold atoms the atomic quasi-clusters will transport in the lattice potential with a uniform current density. Combining equation (10) with the normalization integral as in equation (5) yields the average number of atoms per well

$$N'/n = (n\pi)^{-1} \int_{\pi/2}^{(n+1/2)\pi} R^2(y)dy = (\mu - 1 - V_2/2)/g_0, \quad (11)$$

where N' is the number of atoms in a row of the optical lattices and n the number of lattices. Since the chemical potential has various possible values, the number of atoms per well N'/n may be very large. However, its minimum is limited by the inequality $|\mu - 1| \geq |V_2|$. Employing the parameter set $\mu = 12,\ V_2 = 8,\ g_0 = 8\pi ka = 1.02$, from equation (10) we numerically plot the particle-number density $R^2(y)$ versus y in Figure 5 as a solid curve. This curve shows that the number density does not vanish over the optical potential (the dashed line). In Figure 6 we show the spatial evolution of the superfluid velocity (in units of mm/s) for $\mu = 12,\ g_0 = 1.02$, where the solid, dashed and dotted curves correspond to parameters $V_2 = 5,\ 8$ and 10 respectively. Although a larger V_2 is associated with a larger amplitude, the average velocity over a spatial period

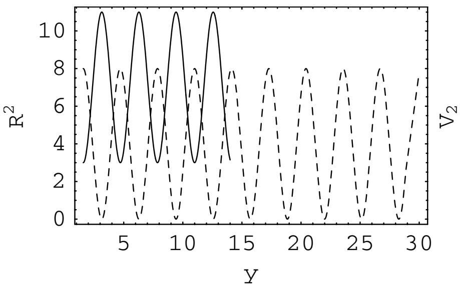

Fig. 5. Plot of the spatial evolution of the particle number density R^2 for a quasi-1D superfluid with parameters $V_2 = 8$, $\mu = 12$, $g_0 = 1.02$. The density does not vanish wherever that implies tunneling of the potential barriers and propagation of the atomic quasi-clusters with the velocity proportional to the phase gradient. The dashed curve indicates the corresponding optical potential.

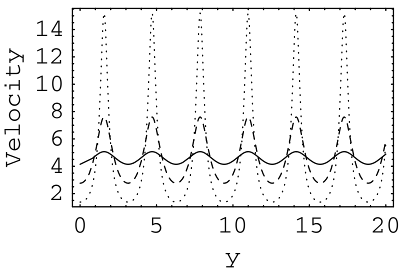

Fig. 6. Plot of the propagation velocity (in units of mm/s) versus spatial coordinate. The chemical potential is fixed as $\mu = 12$ and the trap depth is changed. The solid, dashed and dotted curves correspond to $V_2 = 5$, 8, 10 respectively. The velocity periodically varies with a period 2π and variable amplitude. The larger V_2 is associated with the larger amplitude, but the mean velocity is invariable.

2π is the same for different V_2. If we adopt the laser with wavelength $\lambda = 2\pi/k \approx 1$ μm and the ^{87}Rb atoms with mass m being 87 times the proton mass, the average velocity reads

$$\overline{v} = (2\pi)^{-1} \int_0^{2\pi} (k\hbar\Theta_y/m)dy = 4.58259(\text{mm/s}). \quad (12)$$

Now let us see how one can adopt the optical brake to operate the atomic quasi-clusters. It is known that if the lattice potential depth $|V_2|$ is adjusted to be sufficiently large, no atom can tunnel through the potential barrier [13]. This infers the particle-number density vanishing at a peak point $y_j = (j + 1/2)\pi$ for $j = 0, 1, ...$ of the optical potential $V_2 \sin^2 y$ with $V_2 > 0$. Such a critical solution is obtained by increasing the trap depth to the critical value $V_2 = \mu - 1$ and inserting it into equation (10),

$$\psi'(y) = R'(y) = \sqrt{V_2/g_0}\ \cos y \quad \text{for} \quad \mu = 1 + V_2, \quad (13)$$

where $V_2/g_0 > 0$ and the phase vanishes. Consequently, we get zero propagation velocity and successfully stop the motion of atomic quasi-clusters. In other words, by adjusting the trap depth V_2 we have realized the quantum transition from the superfluid to a new insulator, which

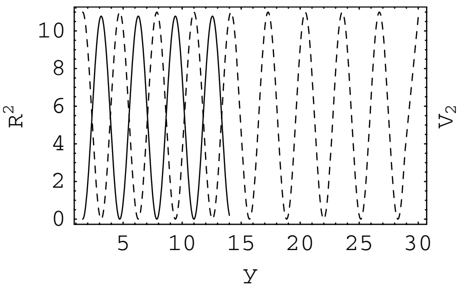

Fig. 7. Plot of the R^2 versus y for $V_2 = 11$ and the same chemical potential and interaction intensity as in Figure 5. It is shown that the increase of well depth leads to the critical insulating state, where the density vanishes at any peak point of the potential (dashed line). This means that the ultracold atomic quasi-clusters are stopped by the optical brake.

is described by the critical state function $\psi'(y)$. Setting $\mu = 12$, $V_2 = 11$ and $g_0 = 1.02$, we plot the spatial evolution of R'^2 in Figure 7 as the solid curve, where the dashed line denotes the corresponding optical potential. Differing from the superfluid state in Figure 5, the particle number density of the insulating state vanishes at any peak point of the potential which means no atoms cross the barriers. Given the chemical potential $\mu = 1 + V_2$, the average number of atoms per well is determined by the experimental parameters V_2 and g_0 through the normalization integral equation (11),

$$N'/n = V_2/(2g_0). \quad (14)$$

For the fixed number of atoms per well and g_0 this gives maximum V_2 and indicates the range of V_2 values in terms of the experimental parameters N', n and g_0, namely the ratio of the trap depth to the interatomic interaction intensity V_2/g_o being less than or equal to two times the atomic number per well $2N'/n$. Since equation (13) is invalid for the Mott insulating state and the invalidation is associated with $V_2 > \mu - 1$, in the Mott insulating state the trap depth will exceed the limit of equation (14) for given number of atoms per well. Substituting the experimental parameters $N'/n \approx 2.5$, $g_0 = 1.02$ into equation (14) leads to the critical trap depth transiting to state (13) as $V_2 = 5.1$, which is less than and approximately equal to the critical value of the Mott insulating state [13], as we have asserted. Due to the reversible quantum transition, we can redrive the atomic quasi-clusters by reducing the optical potential depth to $|V_2| < \mu - 1$ such that equation (10) is again valid.

4 Conclusion

We have obtained four exact solutions of the 2D stationary state GPE by regulating the standing waves of the laser to balance the atom-atom interaction. We analytically and numerically revealed that setting a larger optical potential barrier in one direction can reduce the 2D GPE and its exact solutions to quasi-1D ones. These exact solutions describe the motions of some ultracold atomic quasi-clusters with velocities being proportional to phase gradients of the solutions. When the velocity does not vanish, the atomic quasi-clusters are in the superfluid state, and zero velocity corresponds to the critical insulating state of the system, where the GPE is just validated and the coherent phase becomes incoherent. The ultracold atomic quasi-clusters can be operated theoretically through the exact solutions and experimentally by adjusting the laser beams. Such optical operations will be useful for making an atomic laser of the superfluid [33–35], and performing quantum computations in the insulator.

The exact solutions are some special solutions characterized by different chemical potentials. Given a chemical potential, an exact solution exists only for some particular parameters which satisfy a relationship among the trap depth, the number of atoms per well and the interatomic interaction intensity. This relationship indicates that the critical trap depth is the cause of the quantum phase transitions between the superfluid and the critical insulator. When this relationship breaks down, the system may enter other superfluid states or the Mott insulating state, which can be described by the Bose-Habbard model. On the other hand, we have only considered the zero temperature case in above work. Further work should contain the investigation of thermal fluctuations for finite temperatures [36].

This work was supported by the National Natural Science Foundation of China under Grant No. 10275023, and by the Hubei Provincial Key Laboratory of Gravitational and Quantum Physics of China.

References

1. G. Raithel, G. Birkl, A. Kastberg, W.D. Phillips, S.L. Rolston, Phys. Rev. Lett. **78**, 630 (1997)
2. T. Müller-Seydlitz, M. Hartl, B. Brezger, H. Hansel, C. Keller, A. Schnetz, R.J.C. Spreeuw, T. Pfau, J. Mlynek, Phys. Rev. Lett. **78**, 1038 (1997)
3. M. Greiner, I. Bloch, O. Mandel, T.W. Hänsch, T. Esslinger, Phys. Rev. Lett. **87**, 160405 (2001)
4. S.E. Hamann, D.L. Haycock, G. Klose, P.H. Pax, I.H. Deutsch, P.S. Jessen, Phys. Rev. Lett. **80**, 4149 (1998)
5. K.I. Petsas, A.B. Coates, G. Grynberg, Phys. Rev. A **50**, 5173 (1994)
6. L. Guidoni, P. Verkerk, Phys. Rev. A **57**, R1501 (1998)
7. I.H. Deutsch, P.S. Jessen, Phys. Rev. A **57**, 1972 (1998)
8. M.P.A. Fisher et al., Phys. Rev. B **40**, 546 (1989)
9. W. Krauth, M. Caffarel, J.P. Bouchard, Phys. Rev. B **45**, 3137 (1992)
10. A.P. Kampf, G.T. Zimanyi, Phys. Rev. B **47**, 279 (1993)
11. J.K. Freericks, H. Monien, Europhys. Lett. **26**, 545 (1994)
12. D. Jaksch, C. Bruder, J.I. Cirac, C.W. Gardiner, P. Zoller, Phys. Rev. Lett. **81**, 3108 (1998)
13. M. Greiner, O. Mandel, T. Esslinger, T.W. Hänsch, I. Bloch, Nature **415**, 39 (2002)
14. F. Dalfovo, S. Giorgini, L.P. Pitaevskii, S. Stringari, Rev. Mod. Phys. **71**, 463 (1999)
15. A.J. Leggett, Rev. Mod. Phys. **73**, 307 (2001)
16. B.P. Anderson, M.A. Kasevich, Science **282**, 1686 (1998)
17. C. Orzel, A.K. Tuchman, M.L. Fenselau, M. Yasuda, M.A. Kasevich, Science **291**, 2386 (2001)
18. F.S. Cataliotti, S. Burger, C. Fort, P. Maddaloni, F. Minardi, A. Trombettoni, A. Smerzi, M. Inguscio, Science **293**, 843 (2001)
19. A. Trombettoni, A. Smerzi, Phys. Rev. Lett. **86**, 2353 (2001)
20. J.C. Bronski, L.D. Carr, B. Deconinck, J.N. Kutz, Phys. Rev. Lett. **86**, 1402 (2001)
21. B. Deconinck, B.A. Frigyik, J.N. Kutz, Phys. Lett. A **283**, 177 (2001)
22. J.C. Bronski, L.D. Carr, B. Deconinck, J.N. Kutz, K. Promislow, Phys. Rev. E **63**, 036612 (2001); J.C. Bronski, L.D. Carr, R. Carretero-Gonzalez, B. Deconinck, J.N. Kutz, K. Promislow, Phys. Rev. E **64**, 056615 (2001)
23. S. Liu, H. Xiong, Z. Xu, G. Huang, J. Phys. B: At. Mol. Opt. Phys. **36**, 2083(2003)
24. D. van Oosten, P. van der Straten, H.T.C. Stoof, Phys. Rev. A **63**, 053601 (2001)
25. D. Jaksch et al., Phys. Rev. Lett. **82**, 1975 (1999)
26. W. Hai, C. Lee, G. Chong, L. Shi, Phys. Rev. E **66**, 026202 (2002); C. Lee, W. Hai, L. Shi, X. Zhu, K. Gao, Phys. Rev. A **64**, 053604 (2001).
27. J.R. Anglin, W. Ketterle, Nature **416**, 211 (2002)
28. L.M. Kuang, Z.W. Ouyang, Phys. Rev. A **62**, 023610 (2000)
29. D. Diakonov, L.M. Jensen, C.J. Pethick, H. Smith, Phys. Rev. A **66**, 013604 (2002)
30. E. Tiesinga, B.J. Verhaar, H.T.C. Stoof, Phys. Rev. A **47**, 4114 (1993)
31. S. Inouye et al., Nature **392**, 151 (1998)
32. K.E. Strecker, G.B. Partridge, A.G. Truscott, R.G. Hulet, Nature **417**, 150 (2002)
33. M.R. Andrews, C.G. Townsend, H.J. Miesner, D.S. Durfee, D.M. Kurn, W. Ketteerle, Science **275**, 637 (1997)
34. Y. Wu, X. Yang, Phys. Rev. A **62**, 013603 (2000)
35. J. Stenger et al., Nature **396**, 345 (1998)
36. Yu. Kagan et al., Phys. Rev. A **61**, 045601 (2000)